

## Perpendicular magnetic anisotropy in the Heusler alloy $\text{Co}_2\text{TiSi}/\text{GaAs}(001)$ hybrid structure

M. T. Dau, B. Jenichen, and J. Herfort

Citation: *AIP Advances* **5**, 057130 (2015);

View online: <https://doi.org/10.1063/1.4921237>

View Table of Contents: <http://aip.scitation.org/toc/adv/5/5>

Published by the [American Institute of Physics](#)

---

### Articles you may be interested in

[Structural properties of  \$\text{Co}\_2\text{TiSi}\$  films on  \$\text{GaAs}\(001\)\$](#)

*Journal of Applied Physics* **120**, 225304 (2016); 10.1063/1.4971344

[Effect of disorder on the magnetic and electronic structure of a prospective spin-gapless semiconductor  \$\text{MnCrVAI}\$](#)

*AIP Advances* **7**, 056402 (2016); 10.1063/1.4972797

[Perpendicular magnetic anisotropy in  \$\text{Mn}\_2\text{CoAl}\$  thin film](#)

*AIP Advances* **6**, 015006 (2016); 10.1063/1.4939934

[Structural disorder and magnetism in the spin-gapless semiconductor  \$\text{CoFeCrAl}\$](#)

*AIP Advances* **6**, 056304 (2016); 10.1063/1.4943306

[Spin-filter and spin-gapless semiconductors: The case of Heusler compounds](#)

*AIP Advances* **6**, 055606 (2016); 10.1063/1.4943761

[Investigation of spin-gapless semiconductivity and half-metallicity in  \$\text{Ti}\_2\text{MnAl}\$ -based compounds](#)

*Applied Physics Letters* **108**, 141901 (2016); 10.1063/1.4945600

---

# HAVE YOU HEARD?

Employers hiring scientists and engineers trust

**PHYSICS TODAY | JOBS**

[www.physicstoday.org/jobs](http://www.physicstoday.org/jobs)



## Perpendicular magnetic anisotropy in the Heusler alloy $\text{Co}_2\text{TiSi}/\text{GaAs}(001)$ hybrid structure

M. T. Dau,<sup>a</sup> B. Jenichen, and J. Herfort

*Paul-Drude-Institut für Festkörperelektronik, Hausvogteiplatz 5-7, D-10117 Berlin, Germany*

(Received 13 March 2015; accepted 5 May 2015; published online 13 May 2015)

Investigation of the thickness dependence of the magnetic anisotropy in  $B2$ -type  $\text{Co}_2\text{TiSi}$  films on  $\text{GaAs}(001)$ , shows a pronounced perpendicular magnetic anisotropy at 10 K for thicknesses up to 13.5 nm. We have evidenced that the interfacial anisotropy induced by interface clusters has a strong influence on the perpendicular magnetic anisotropy of this hybrid structure, especially at temperatures lower than the blocking temperature of the clusters (28 K). However, as this influence can be ruled out at higher temperatures, the perpendicular magnetic anisotropy which is found to persist up to room-temperature can be ascribed to the magnetic properties of the  $\text{Co}_2\text{TiSi}$  films. For thicknesses larger than 15.0 nm, we observe an alignment of the magnetic easy axis parallel to the sample surface, which is most likely due to the shape anisotropy and the film structure. © 2015 Author(s). All article content, except where otherwise noted, is licensed under a Creative Commons Attribution 3.0 Unported License. [<http://dx.doi.org/10.1063/1.4921237>]

### INTRODUCTION

Perpendicular magnetic anisotropy (PMA) in ferromagnetic films where the easy axis of magnetization is oriented out-of-plane, is of great interest for realizing perpendicular magnetic tunnel junctions. Such junctions are used in devices with high processing speed and high-density non-volatile memory.<sup>1-3</sup> In addition, the implementation of perpendicularly magnetized thin films in semiconductor-based spintronic devices, for example, in a spin-light emitting diode (spin-LED) has been recently demonstrated as a potential approach to achieve an efficient transfer of spin-polarized current into semiconducting channels.<sup>4,5</sup> However, those devices suffer from the requirement of a large applied magnetic field to turn the magnetic moment out of the sample surface.

Ferromagnetic films with PMA are not commonly observed due to the long-range dipolar interactions or the shape effect. The well-known PMA materials are magnetic alloys containing rare-earth, noble or transition metals. For instance, granular films as well as amorphous films based on  $\text{CoPt}$ ,  $\text{FePt}$ ,  $\text{CoCr}$ ,  $\text{TbFe}$  exhibit a pronounced PMA.<sup>6-9</sup> Nevertheless, potential applications of such materials are limited because of their low crystalline quality. Another widespread PMA material class is metallic stacking layers that are also based on transition, noble metals and rare-earth magnets.<sup>10,11</sup> The PMA of these structures has an interfacial origin for which the orbital hybridization and/or the intermixing at the interface promotes the perpendicular spin coupling.<sup>12,13</sup> Since metallic layers should be thin enough for triggering the PMA, the fabrication process of such multilayers and the related devices would be more complicated than a simple layer.

In the last decade, the growth and characterization of full Heusler alloy (FHA) films have been intensely investigated because many of them have been theoretically predicted to have a fully spin-polarized conduction band.<sup>14-17</sup> The intrinsic magnetic anisotropy of the well-known FHA films has been found to be dominated by the in-plane anisotropy.<sup>16-18</sup> Very recently, the interface-induced PMA was discovered in a Co-based FHA ( $\text{Co}_2\text{FeAl}$ ) in contact with a  $\text{MgO}$  oxide layer.<sup>19,20</sup> The proposed explanation for the PMA is similar to that of  $\text{CoFeB}$  or  $\text{Fe}/\text{MgO}$  systems for which interfacial anisotropy induced by hybridization of Fe-, Co- $3d$  and O- $2p$  orbitals causes the

---

<sup>a</sup>Electronic email: [dau@pdi-berlin.de](mailto:dau@pdi-berlin.de)

PMA.<sup>3,21</sup> For a hybrid structure based on a very thin FHA film (on the order of a few angstroms) coupled with a MgO barrier, a question is whether chemical interactions will alter the electronic band structure of the FHA, (i. e., its spin polarization). Furthermore, film oxidation arising from excess oxygen makes the control of such an interface relatively difficult. Therefore, it is desired to acquire a PMA FHA film with easy-to-adjust thickness in order to maintain its intrinsic high spin polarization and perpendicular magnetization properties. In this study, we report on the observation of PMA in FHA Co<sub>2</sub>TiSi/GaAs hybrid structures for thicknesses up to 13.5 nm, which is one order of magnitude higher than that previously reported for of PMA ultra-thin films.<sup>3,19,21</sup> For higher thicknesses, the in-plane magnetic anisotropy dominates and the easy axis of magnetization is thus found to be in-plane.

## EXPERIMENTAL

All the Co<sub>2</sub>TiSi films were grown on semi-insulating (001)-oriented GaAs substrates. A 400-nm-thick GaAs buffer layer was grown in a III-V semiconductor growth chamber to ensure a single-crystal surface free of contaminants and defects. The Co<sub>2</sub>TiSi films were subsequently synthesized in an As-free chamber for metal growth after a transfer under ultra-high vacuum. The films were grown at 360 °C, which is within the optimum range of the growth temperature as previously reported.<sup>22</sup> Accordingly, the film grown at 360 °C crystallizes predominantly in *B2* order, the Curie temperature is around room-temperature (RT) with an average magnetic saturation of 0.8 μ<sub>B</sub>. A detailed description of the film properties as well as the film stoichiometry determination can be found in Ref. 22. For this study, *in-situ* reflection high energy electrons diffraction (RHEED) was used for monitoring the film surface during the growth (not shown here). The in-plane epitaxial relationship with respect to the cubic symmetry of the GaAs surface was found to be unchanged for all the films ([110]Co<sub>2</sub>TiSi // [110]GaAs). For film thicknesses below 15.0 nm, streaky RHEED patterns are observed. The surfaces are also reconstructed with the occurrence of one-half streaks along the [100] azimuth. These reconstructed streaks, corresponding to the (2x1) Co<sub>2</sub>TiSi surface, persist throughout the deposition. As the thickness is increased, the RHEED patterns become spottier and a strong diffused background is observed. This clearly indicates a degradation of the thick-film surfaces. The cross-sectional interface film/substrate was characterized by high resolution transmission electron microscopy (HRTEM) using a JEOL 3010 system operating at an accelerated voltage of 200 kV. Magnetic measurements were carried out with a Quantum Design superconducting quantum interference device (SQUID).

## RESULTS AND DISCUSSION

The thickness dependence of the in-plane and perpendicular magnetic anisotropy of the Co<sub>2</sub>TiSi films is presented in Fig. 1. The hysteresis loops were recorded at 10 K and 100 K. They are normalized to the saturation magnetization  $M_S$  and shown together for comparison. The hysteresis curves measured along different in-plane crystallographic axes reveal a very weak anisotropy. Hence, only the data measured along the [110] direction are shown, to exemplify the in-plane magnetic measurements. A transition from out-of-plane to in-plane magnetization of the easy axis can be clearly observed with increasing thickness for both temperatures. However, the perpendicular anisotropy is less pronounced at 100 K. Because the Curie temperature of the Co<sub>2</sub>TiSi films is low, the thermal effect strongly disturbs the magnetic stability of the films. Therefore, in this work, we mostly focus on the perpendicular magnetic anisotropy measured at 10 K. A detailed analysis of the hysteresis loops for a number of films is summarized in Fig. 2. Based on Fig. 1 and Fig. 2, one can clearly distinguish two different regions of magnetic anisotropy with respect to the film thickness. First, for the region with thicknesses smaller than 13.5 nm (PA region) the films exhibit a pronounced PMA. In a narrow thickness range of about 13.5 to 15.0 nm, the magnetic anisotropy is found to be almost identical irrespective of the magnetic field directions. Second, for films thicker than 15.0 nm, the easy axis of magnetization is oriented along the in-plane direction (IA region). The thickness dependence of the squareness of the M-H curves, defined as a ratio of remanence to saturation

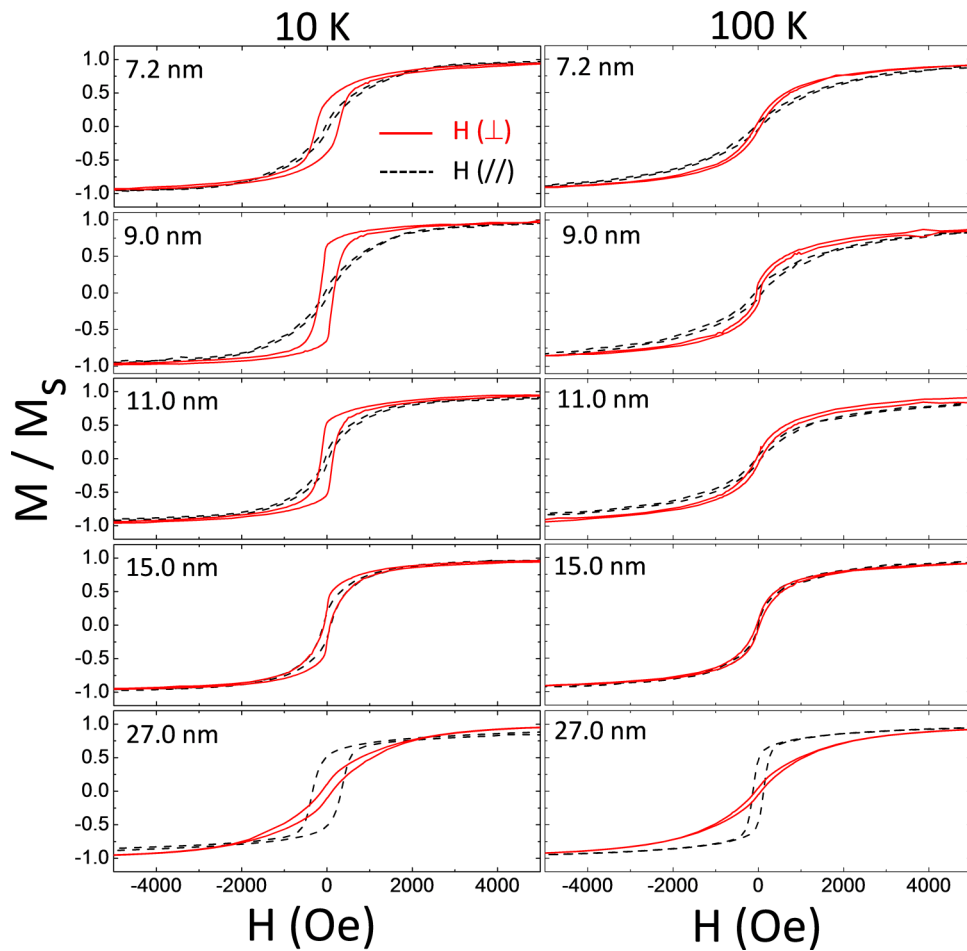


FIG. 1. M-H loops of the  $\text{Co}_2\text{TiSi}$  films with different thicknesses taken at 10 K and 100 K along directions perpendicular [001] and parallel [110] to the sample surface. The diamagnetic contribution of the GaAs substrate was subtracted.

magnetization  $M_r/M_s$ , is shown in Fig. 2(a). Excluding the thicknesses of 5.0 nm and 7.2 nm, the out-of-plane ( $H_\perp$ ) and in-plane ( $H_\parallel$ ) data show two opposite trends, mutually indicating the permutation of the magnetic easy axis. Indeed, the out-of-plane curve exhibits a monotonous decrease of the squareness, while it increases for the in-plane curve with increasing thickness. Further inspection of the region where the thickness is between 9.0 nm and 13.5 nm (PA region) reveals that the out-of-plane squareness decreases rapidly (slope  $s = 0.11 \text{ nm}^{-1}$ ), whereas the in-plane squareness shows a slight increase ( $s = 0.01 \text{ nm}^{-1}$ ). This describes how fast perpendicular magnetic domains disappear under the film thickness effect. On the other hand, a similar evolution of the squareness is found for the IA region. Here, a fast increase of the in-plane squareness and a slight decrease of the out-of-plane squareness are observed. The coercive fields  $H_C$  extracted from the out-of-plane and in-plane hysteresis loops are shown in Fig. 2(b). For the out-of-plane data ( $H_\perp$ ),  $H_C$  sharply decreases from 260 Oe to 83 Oe when the thickness increases from 7.2 nm to 13.5 nm (PA region). However,  $H_C$  increases slightly for the thicker films (IA region). Regarding the in-plane data ( $H_\parallel$ ), an inverse tendency is observed: a slight change of  $H_C$  in the PA region and a notable increase of  $H_C$  above 15.0 nm in the IA region with increasing thickness. Such a behavior of  $H_C$  is similar to that observed in the magnetic switching process of partially ordered FePt thin films.<sup>23</sup> The pinning of perpendicularly magnetic domain walls and/or a limited nucleation of the magnetic domain walls are possible explanations for the thickness dependence of  $H_C$ .<sup>23</sup> Note that we found a distinct decrease of the squareness and  $H_C$  in the PA region for the thinnest films (5-, 7-nm-thick films). This may be associated with interfacial states where precipitates or intermixing products have a

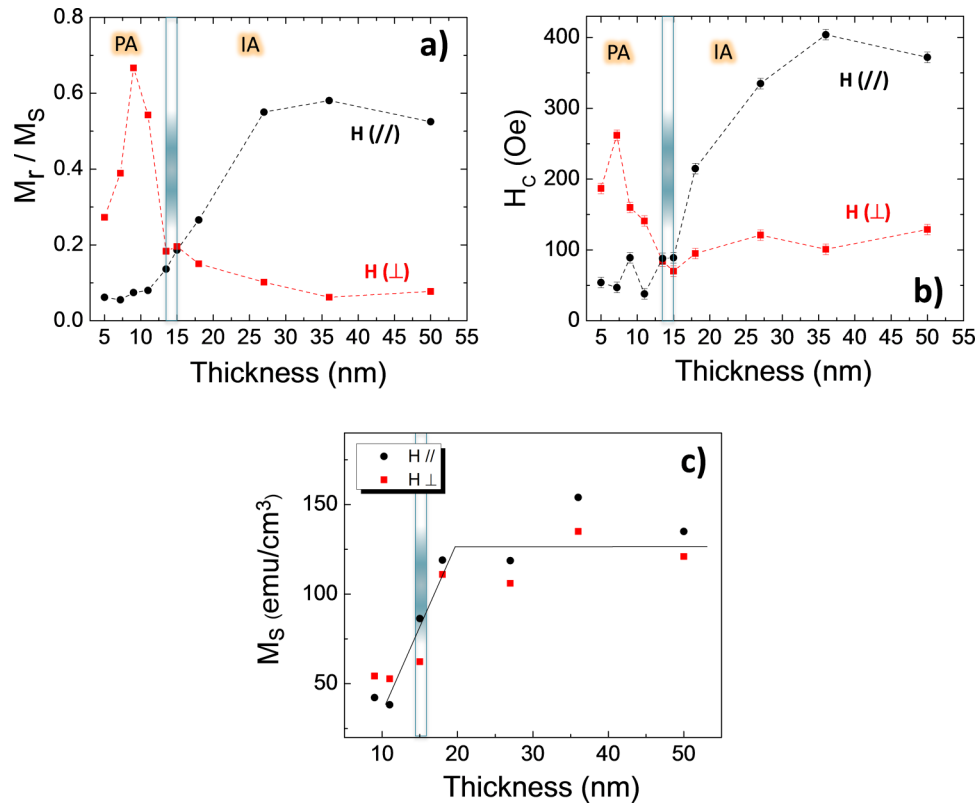


FIG. 2. (a) Squareness  $M_r/M_s$ , (b)  $H_c$  and (c) Saturation magnetization  $M_s$  obtained from the in-plane and out-of-plane hysteresis loops at 10 K and plotted as a function of the film thickness. PA and IA regions correspond to PMA films and in-plane magnetic anisotropy films, respectively. The solid line in figure (c) is to guide the eyes.

significant contribution to the magnetic properties. The interfacial state, which will be discussed in the following section, may also affect the saturation magnetizations of the thinnest films (Fig. 2(c)) since they are remarkably low and anisotropic for the in-plane and out-of-plane measurements. However, the interfacial contribution to the saturation magnetization becomes negligible when the thickness is above 15.0 nm.

The resulting data have clearly shown that  $\text{Co}_2\text{TiSi}$  films with perpendicular magnetization can be obtained for thicknesses as large as 13.5 nm. This value is one order of magnitude larger than that of other films with an interface-induced PMA, such as  $\text{CoFeB}$ ,  $\text{Co}_2\text{FeAl}$  and  $\text{Fe}$ .<sup>3,19,21</sup> For these films, a tremendous reduction in thickness was required in order to alleviate the magneto-crystalline anisotropy with respect to the interface anisotropy. Nevertheless, the origin of PMA in the  $\text{Co}_2\text{TiSi}/\text{GaAs}$  system must be different nature because of the large thickness range. In fact, interfacial anisotropy induced by *sp-d* hybridization between localized moments of Co and of Ga and As atoms can be ruled out, because the interfacial hybridization is not a long-range effect and would concern only a thickness of above a dozen of Å, much less than the thickness range of our  $\text{Co}_2\text{TiSi}$  films.<sup>3,19,21</sup> Another source of interfacial anisotropy possibly comes from the presence of interface precipitates due to intermixing, diffusion or interface reactions. In order to clarify this point, cross-sectional TEM studies were systematically performed. Figure 3(a) depicts the interface structure of a 36-nm-thick  $\text{Co}_2\text{TiSi}$  film and the GaAs substrate, showing regions where the reactions occur at the interface. These regions in cross-section (hereafter called interface clusters) are mostly oval-shaped with bimodal size distribution: about 20 nm and 40 nm in length, 10 nm in depth. This size distribution is comparable with that of clusters detected at the  $\text{Co}_2\text{FeSi}/\text{GaAs}$  interface in the low temperature growth regime.<sup>24</sup> A detailed analysis of a fast Fourier transform on the clusters (not shown) reveals that they exhibit a diamond cubic symmetry, i. e. a counterpart of the zincblende GaAs lattice, with a similar interplanar spacing. For the growth temperature of



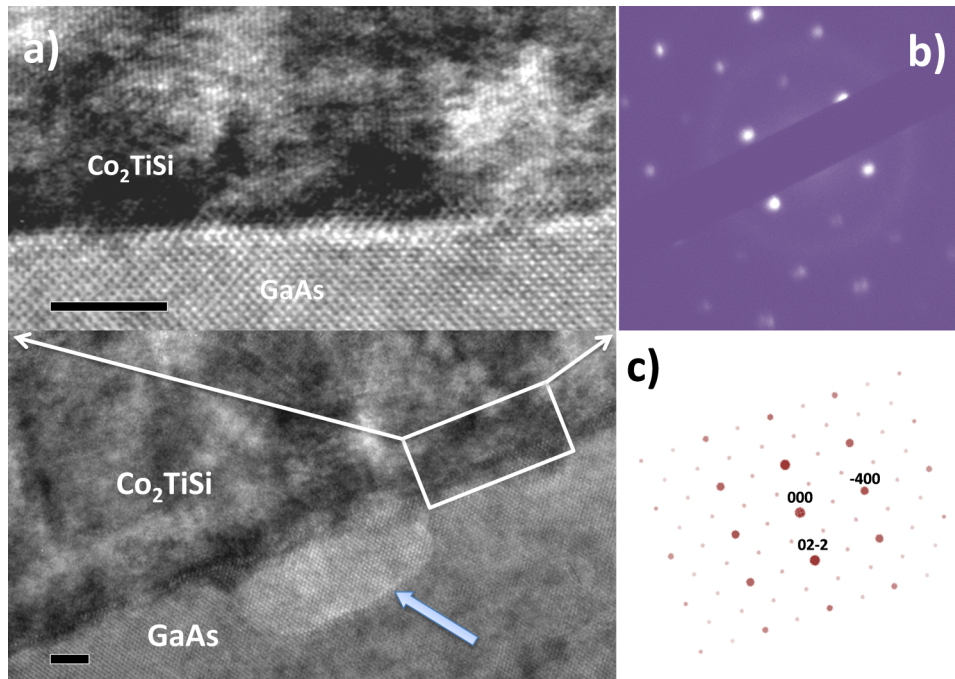


FIG. 3. (a) Cross-sectional TEM micrographs of the interface  $\text{Co}_2\text{TiSi}/\text{GaAs}$  with a typical interfacial cluster (indicated by the arrow). The scale bars correspond to 5 nm. (b) SAED of the  $\text{Co}_2\text{TiSi}$  film taken with the zone axis  $[110]$ . (c) Kinetic simulation of diffraction peaks of the  $\text{Co}_2\text{TiSi}$  lattice obtained with the zone axis  $[110]$ .

360 °C, it is known that metallic elements from the  $\text{Co}_2\text{TiSi}$  films may chemically react with the GaAs substrates giving rise to interfacial products. Co-based or Ti-based phases such as  $\text{Co}_2\text{GaAs}$ ,  $\text{CoAs}$ ,  $\text{TiAs}$ ,  $\text{Ti}_{1-x}\text{Ga}_x$  might be formed in this condition.<sup>24,26</sup> However, these have either an orthorhombic or hexagonal structure with a different lattice constant from that of GaAs.<sup>25,26</sup> We note that the x-ray diffraction scans did not show any additional peaks besides those of  $\text{Co}_2\text{TiSi}$  and GaAs. Therefore, these findings strongly suggest that interface clusters originate from the in-diffusion of the  $\text{Co}_2\text{TiSi}$  film into the substrate rather than from chemical reactions. An inspection by electron energy loss spectroscopy (EELS) (not shown) also evidenced the incorporation of Co and Ti in these clusters, resulting in dilute Co and Ti clusters. The selected area electron diffraction (SAED) pattern of the film in the vicinity of the interface area, and the simulated pattern, are shown in the Fig. 3(b) and 3(c), respectively. The diffraction peaks of the SAED pattern are identical to those of the simulated pattern, confirming the typical cubic lattice of  $\text{Co}_2\text{TiSi}$  with long-range crystallinity and order. Apart from the clusters and the film quality in the interface area, we observe polycrystalline and amorphous regions which are mostly located in the upper part of the film (about 20 nm from the interface). This is actually consistent with the degradation of the RHEED patterns with increasing film thickness. We emphasize that the interesting information obtained from the TEM investigation is the presence of clusters at the interface which can be apparently expected for the whole range of thickness studied.

An obvious question is how the clusters affect the magnetic properties of the films. Indeed, these clusters, which contain magnetic Co ions, may be considered as diluted magnetic clusters.<sup>27</sup> Clearly, they possess their own magnetic moments which should have a significant impact on the squareness, the  $H_C$  and the saturation magnetization of the films for a film thickness less than 15.0 nm as mentioned above. In addition, because of their inherent magnetic anisotropy, they could promote the PMA of these films. Figure 4 shows zero-field cooled – field cooled (ZFC-FC) curves of the 9-nm-thick film (a PMA film) with an external magnetic field of 50 Oe applied parallel and perpendicular to the sample surface. The superparamagnetic state of the clusters is found only for the perpendicular configuration with a blocking temperature  $T_B \sim 28$  K estimated from the peak of the ZFC curve. This evidences that the clusters indeed exhibit a magnetic anisotropy with a

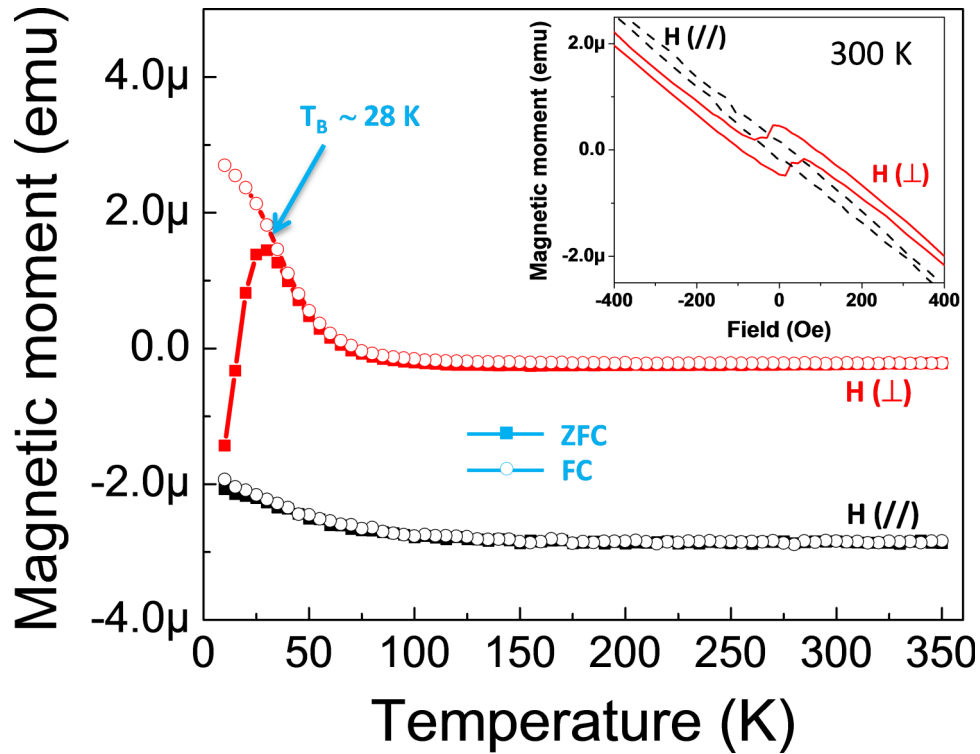


FIG. 4. ZFC-FC curves of the 9-nm-thick PMA film with an external field of 50 Oe applied perpendicular and parallel to the sample surface. The in-plane ZFC-FC data were multiplied by 5 and vertically shifted for clarity. The inset displays the raw in-plane and perpendicular M-H data measured on the same sample at 300 K.

preferentially perpendicular orientation below 28 K. Yet, the clusters will have a paramagnetic state and their magnetic anisotropy can be discarded in case that one carries out the measurements at temperatures higher than  $T_B$ . Indeed, as previously shown in Fig. 1, the perpendicular anisotropy is still preserved at 100 K for the films with thicknesses lower than 15 nm. In addition, the M-H loops measured at 300 K (inset of fig. 4) show that a distinct hysteresis behavior around zero-applied field is observed only for the perpendicular data, indicating the persistence of the perpendicular component at room temperature. Note that the raw data is presented because the subtraction of the diamagnetic signals from the GaAs substrate and any magnetic impurities associated with the substrate is very critical and somehow meaningless at 300 K, especially for the in-plane data. This is due to a significant reduction of the ferromagnetic moment (thermal fluctuation, matter inter-diffusion) and the low signal-to-noise ratio. These findings suggest that the PMA of the  $\text{Co}_2\text{TiSi}/\text{GaAs}$  hybrid structure can be ascribed to the magnetic anisotropy of the  $\text{Co}_2\text{TiSi}$  films. The total PMA of samples obtained for temperatures below  $T_B$  results from both the perpendicular anisotropy of the clusters and that of the  $\text{Co}_2\text{TiSi}$  films.

The intriguing origin of the PMA in the  $\text{Co}_2\text{TiSi}$  films is so far not clear. Figure 5 depicts the XRD scans of the (004) reflection with different film thicknesses. It can be seen that there is no peak shift with varying film thickness, indicating that perpendicular lattice constant  $a_{\perp} = 5.773 \text{ \AA}$  remains unchanged. In an epitaxial heterostructure where misfit is small and both substrate and film are cubic, strain in the film, if it exists, would induce a tetragonal distortion which is characterized by the  $a_{\perp}/a_{\parallel}$  ratio ( $a_{\parallel}$  is in-plane lattice constant). However, assuming that such a tetragonal distortion takes place in our films, the  $a_{\perp}/a_{\parallel}$  ratio is apparently constant when the film thickness varies. This indicates that the strain or magneto-elastic anisotropy would not be associated with the PMA of the  $\text{Co}_2\text{TiSi}$  films. Furthermore, the interfacial anisotropy induced by the hybridization nature of the bonding can be ruled out due to the large film thicknesses. Also, the contribution of the surface roughness to the PMA is practically negligible due to the very low value of the surface roughness (a few  $\text{\AA}$ ) obtained

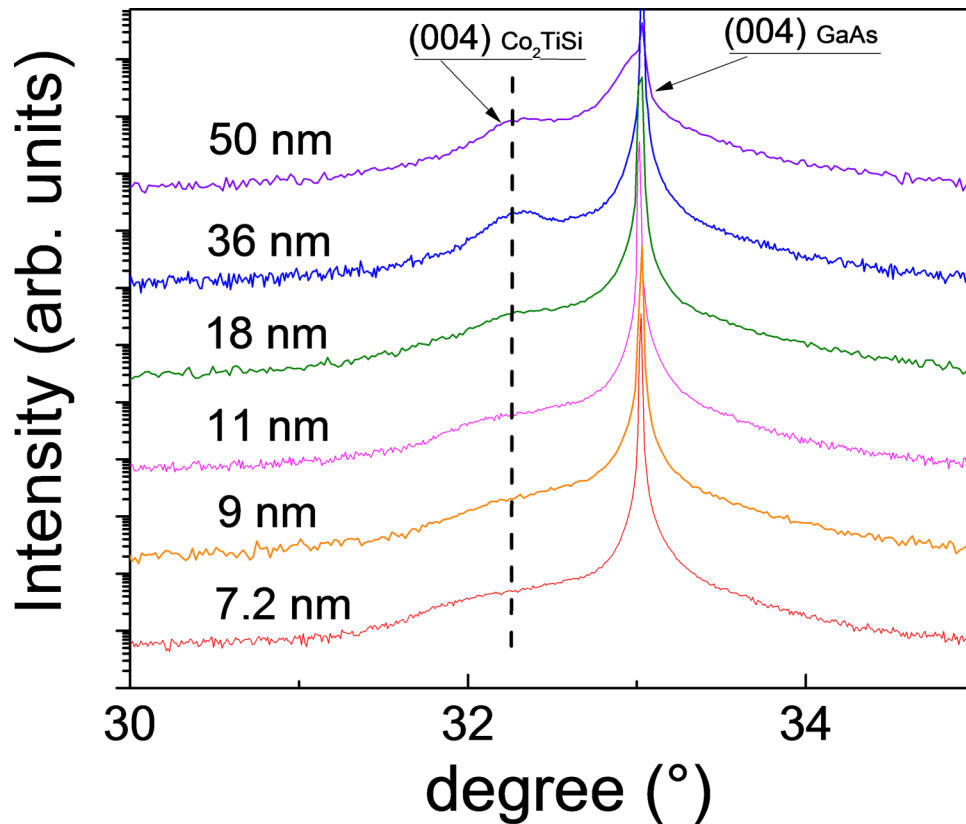


FIG. 5. XRD scans of the (004) peak with different thicknesses.

by AFM, compared to that of the film thickness. Regarding the magnetic structure, one may speculate that the films are composed of magnetic domains, which could mainly possess perpendicular magnetization. For such domains, sub-lattice interactions within the  $\text{Co}_2\text{TiSi}$  would merely depend on the Co atoms. Indeed, contrary to other Heusler  $\text{Co}_2\text{XY}$  films ( $X = \text{Fe}, \text{Mn}, \text{Cr}; Y = \text{Si}$ ) where the magnetic moment of the lattice is both carried by the Co and X atoms, the  $\text{Co}_2\text{TiSi}$  lattice moment is mainly carried by the Co atoms.<sup>28</sup> Therefore, such short-range interactions between localized Co magnetic moments would be stronger in an ordered structure and would promote a dominance of the perpendicular anisotropy.<sup>29</sup> In addition, despite the long-range crystallinity of the films observed from the TEM images, we cannot ignore the role of crystal defects in the films (point defects, boundary grains, etc. . . ), which may act as pinning centers in the interactions between the magnetic domain walls, strengthening the perpendicular anisotropy in the films. When the film thickness increases, the perpendicular-to-parallel transition of the easy axis could be due to the dominance of the shape anisotropy, which tends to align the dipolar interactions, i. e., the magnetization parallel to the plane of the films. Note that a degradation of the film structure and a slight increase of the roughness (from 5.4 Å to 8.8 Å) due to the increase of the film thickness could also affect the strength of the shape anisotropy with respect to other sources of anisotropy.

## CONCLUSION

To summarize, a thickness-dependent magnetic anisotropy study has revealed a perpendicular magnetization for  $\text{Co}_2\text{TiSi}/\text{GaAs}(001)$  hybrid structures with film thicknesses as large as 13.5 nm. We have shown that the interface clusters, which originate from the inter-diffusion, are one possible source of the interfacial anisotropy. The clusters directly affect the perpendicular magnetic anisotropy of the hybrid structure, in particular below the blocking temperature  $T_B$  (28 K) of the



clusters. However, as the perpendicular component persists up to room temperature, well above  $T_B$ , the anisotropy contribution from the clusters can be separated and we can attribute the perpendicular anisotropy to the magnetic properties of the  $\text{Co}_2\text{TiSi}$  films. These results open up promising perspectives of the  $\text{Co}_2\text{TiSi}/\text{GaAs}$  hybrid structures not only for spin transport in semiconductor devices at remanence, but also for oxide-based magnetic tunnel junctions with perpendicularly magnetized electrodes.

## ACKNOWLEDGEMENTS

The authors would like to thank Claudia Hermann for MBE assistance, Doreen Steffen for sample preparation and Xiang Kong for EELS measurements. The authors gratefully acknowledge the critical reading of Yukihiko Takagaki. This work was supported by the German DFG within the priority program SPP 1538.

- <sup>1</sup> M. Albrecht, C. T. Rettner, A. Moser, M. E. Best, and B. D. Terris, *Appl. Phys. Lett.* **81**, 2875 (2002).
- <sup>2</sup> A. D. Kent, B. Özyilmaz, and E. Del Barco, *Appl. Phys. Lett.* **84**, 3897 (2004).
- <sup>3</sup> S. Ikeda, K. Miura, H. Yamamoto, K. Mizunuma, H. D. Gan, M. Endo, S. Kanai, J. Hayakawa, F. Matsukura, and H. Ohno, *Nat. Mat.* **9**, 721 (2010).
- <sup>4</sup> M. Ramsteiner, O. Brandt, T. Flissikowski, H. T. Grahn, M. Hashimoto, J. Herfort, and H. Kostial, *Phys. Rev. B* **78**, 121303 (2008).
- <sup>5</sup> R. Farshchi, M. Ramsteiner, J. Herfort, A. Tahraoui, and H. T. Grahn, *Appl. Phys. Lett.* **98**, 162508 (2011).
- <sup>6</sup> S. Jeong, Y.-N. Hsu, D. E. Laughlin, and M. E. McHenry, *IEEE Trans. Magn.* **36**, 2336 (2000).
- <sup>7</sup> T. Shima, K. Takanashi, Y. K. Takahashi, and K. Hono, *Appl. Phys. Lett.* **85**, 2571 (2004).
- <sup>8</sup> H. Van Kranenburg, J. C. Udder, Y. Maeda, L. Toth, and Th. J. A. Popma, *IEEE Trans. Magn.* **26**, 1620 (1990).
- <sup>9</sup> V. G. Harris and T. Pokhil, *Phys. Rev. Lett.* **87**, 067207 (2001).
- <sup>10</sup> F. Richomme, J. Teillet, A. Fnidiki, and W. Keune, *Phys. Rev. B* **64**, 094415 (2001).
- <sup>11</sup> M. Gottwald, K. Lee, J. J. Kan, B. Ocker, J. Wrona, S. Tibus, J. Langer, S. H. Kang, and E. E. Fullerton, *Appl. Phys. Lett.* **102**, 052405 (2013).
- <sup>12</sup> M. T. Johnson, P. J. H. Bloemen, F. J. A. den Broeder, and J. J. de Vries, *Rep. Prog. Phys.* **59**, 1409 (1996).
- <sup>13</sup> N. Nakajima, T. Koide, T. Shidara, H. Miyauchi, H. Fukutani, A. Fujimori, K. Iio, and T. Katayama, *Phys. Rev. Lett.* **81**, 5229 (1998).
- <sup>14</sup> S. J. Hashemifar, P. Kratzer, and M. Scheffler, *Phys. Rev. Lett.* **94**, 096402 (2005).
- <sup>15</sup> V. Koa, G. Hana, and Y.P. Feng, *J. Magn. Magn. Mater.* **322**, 2989 (2010).
- <sup>16</sup> T. Ambrose, J. J. Krebs, and G. A. Prinz, *Appl. Phys. Lett.* **76**, 3280 (2000).
- <sup>17</sup> M. Hashimoto, J. Herfort, H.-P. Schönherr, and K. H. Ploog, *Appl. Phys. Lett.* **87**, 102506 (2005).
- <sup>18</sup> M. Belmeguenai, F. Zighem, D. Faurie, H. Tuzcuoglu, S.-M. Chérif, P. Moch, K. Westerholt, and W. Seiler, *Phys. Status Solidi A* **209**, 1328 (2012).
- <sup>19</sup> Z. Wen, H. Sukegawa, S. Mitani, and K. Inomata, *Appl. Phys. Lett.* **98**, 242507 (2011).
- <sup>20</sup> Y. Cui, B. Khodadadi, S. Schäfer, T. Mewes, J. Lu, and S. A. Wolf, *Appl. Phys. Lett.* **102**, 162403 (2013).
- <sup>21</sup> J. W. Koo, S. Mitani, T. T. Sasaki, H. Sukegawa, Z. C. Wen, T. Ohkubo, T. Niizeki, K. Inomata, and K. Hono, *Appl. Phys. Lett.* **103**, 192401 (2013).
- <sup>22</sup> M. T. Dau and J. Herfort, *J. Phys. D: Appl. Phys.* **48**, 025003 (2015).
- <sup>23</sup> V. Gehanno, R. Homann, Y. Samson, A. Marty, and S. Auret, *Eur. Phys. J. B* **10**, 457 (1999).
- <sup>24</sup> M. Hashimoto, J. Herfort, A. Trampert, H-P Schönherr, and K. H. Ploog, *J. Phys. D: Appl. Phys.* **40**, 1631 (2007).
- <sup>25</sup> C. J. Palmström, C. C. Chang, A. Yu, G. J. Galvin, and J. W. Mayer, *J. Appl. Phys.* **62**, 3755 (1987).
- <sup>26</sup> K. B. Kim, M. Kniffin, R. Sinclair, and C. R. Helms, *J. Vac. Sci. Technol. A* **6**, 1473 (1988).
- <sup>27</sup> H. Ohno, A. Shen, F. Matsukura, A. Oiwa, A. Endo, S. Katsumoto, and Y. Iye, *Appl. Phys. Lett.* **69**, 363 (1996).
- <sup>28</sup> X. Q. Chen, R. Podlucky, and P. Rogl, *J. Appl. Phys.* **100**, 113901 (2006).
- <sup>29</sup> G. Suran, K. Ounadjela, and F. Machizaud, *J. Appl. Phys.* **61**, 3658 (1987).